

The Implications of Tropical Rossby Waves for Tropical Tropopause Cirrus Formation and for the Equatorial Upwelling of the Brewer–Dobson Circulation

MATTHEW T. BOEHM AND SUKYOUNG LEE

Department of Meteorology, The Pennsylvania State University, University Park, Pennsylvania

(Manuscript received 6 February 2002, in final form 1 July 2002)

ABSTRACT

This study puts forward a mechanism for the observed upwelling in the tropical upper troposphere and lower stratosphere. In this hypothesis, the tropical upwelling is driven by momentum transport by Rossby waves that are generated by tropical convection. To test this hypothesis, model runs are conducted using an axisymmetric, global, primitive equation model. In these runs, the effect of Rossby waves is included by driving the model with observed fields of large-scale eddy momentum flux convergence. The resulting overturning circulation includes both meridional flow from the intertropical convergence zone (ITCZ) to the equator and rising motion in the tropical tropopause transition layer (TTL). This circulation therefore helps to explain the transport of moisture from the lower portion of the TTL in the ITCZ to the equatorial cold-point tropopause, where tropopause cirrus layers frequently occur.

1. Introduction

Remote sensing observations by satellites (Wang et al. 1996; Rossow and Schiffer 1991), ground-based lidars (Mather et al. 1998), and airborne lidars (Winker and Trepte 1998; Jensen et al. 1996b) have revealed the frequent occurrence of thin cirrus layers (tropopause cirrus, hereafter) near the tropical cold-point tropopause at altitudes between 15 and 18 km. These layers generally are several hundred meters to one kilometer in thickness, extend several hundred to more than one thousand kilometers horizontally, and persist for time periods of several hours to several days.

Tropopause cirrus layers impact the radiative balance within the TTL. In general, these layers are radiatively warmed, although it has recently been shown that they can also be radiatively cooled when located above a high, thick anvil (Hartmann et al. 2001). These radiative processes, in turn, have important impacts on the thermal structure and vertical velocity in the upper tropical troposphere (McFarquhar et al. 2000; Hartmann et al. 2001; Rosenfield et al. 1998). In addition, it has been suggested that sedimentation from tropopause cirrus plays an important role in producing the low water vapor mixing ratios observed in the lower stratosphere (Newell and Gould-Stewart 1981; Tsuda et al. 1994; Potter and Holton 1995; Jensen et al. 1996a; Hartmann et al. 2001). Despite their importance to global climate, tropopause cirrus processes are poorly understood, in part

because of an observational shortage of the properties of these clouds (Heymsfield et al. 1998; Heymsfield and McFarquhar 1996; Wang et al. 1996); in situ observation requires specialized aircraft that can operate near the tropical cold-point tropopause at altitudes of 16–18 km and in occasionally turbulent conditions. Such observations are available for only a very small number of cases (Heymsfield 1986; Booker and Stickel 1982).

An important topic related to tropopause cirrus is the source of water vapor near the cold-point tropopause. While it is well established that water vapor is transported from the surface to the tropical upper troposphere primarily by deep convection (Clark et al. 1998; Elson et al. 1996; Sherwood 1999; Salathé and Hartmann 1997), it remains unclear exactly how water vapor reaches the level of the cold-point tropopause. If deep convection consistently reaches the cold-point tropopause over a large portion of the Tropics, then ice crystals and water vapor detrained from convective clouds can act directly as the required moisture source. If, on the other hand, deep convection generally detrains well below the cold-point tropopause, then additional moisture transport is required.

While there are observations of convection penetrating to the tropical cold-point tropopause and even into the lower stratosphere (Kley et al. 1982; Knollenberg et al. 1982; Ebert and Holland 1992; Ackerman et al. 1988; Danielsen 1993; Schmetz et al. 1997; Simpson et al. 1998), reported cases of such convection have been primarily either associated with a tropical cyclone or else from convectively favored regions, most frequently the maritime continent region of the western Pacific

Corresponding author address: Dr. Matthew T. Boehm, NASA Goddard Space Flight Center, Code 912, Greenbelt, MD 20771.
E-mail: boehm@agnes.gsfc.nasa.gov

Ocean. This convection, therefore, is not representative of typical conditions throughout most of the Tropics. Instead, observations and model results suggest that in most of the Tropics during most of the year tropical convection is generally capped 2–4 km below the cold-point tropopause, with only very infrequent penetration to that level (Gettelman et al. 2002; Graves 1951; Defant and van de Boogaard 1963; Palmén and Newton 1969; Thuburn and Craig 1997; Forster et al. 1997; Highwood and Hoskins 1998; Folkins et al. 1999; Keith 2000). In particular, Gettelman et al. (2002) estimated that the annual average over all longitudes in the Tropics of the timescale on which tropical convection replaces the mass at a given altitude increases from 1 month at 12 km to 1 yr at 16 km to 4 yr at an altitude of 18 km. Because convection takes on the order of 1 yr to replace the air at the cold-point tropopause, it is unlikely that tropical convection acting alone is able to supply the moisture required to explain the high frequency with which tropopause cirrus is observed over much of the Tropics.

As an alternative explanation, it has been proposed that gentle, large-scale rising motion in the upper tropical troposphere plays an important role in the vertical transport of moisture from the altitude at which it is detrained from convection to the cold-point tropopause (Sherwood and Dessler 2000, 2001). There indeed exists observational evidence of such gentle, large-scale rising motion. A variety of indirect measurements and estimates (Rosenlof 1995; Eluszkiewicz et al. 1996; Rosenlof and Holton 1993; Seol and Yamazaki 1999; Mote et al. 1996, 1998; Niwano and Shiotani 2001; Hall and Waugh 1997; Boering et al. 1996) find the zonal mean vertical velocity near the tropical tropopause to be 0.2–0.4 mm s⁻¹. The possibility of gentle upwelling playing the primary role in vertical moisture transport is consistent with the recent finding (Comstock et al. 2002, Manuscript submitted to *J. Geophys. Res.*, hereafter CAM) that the tropical ice crystals in tropopause cirrus are radically different from those in cirrus anvils detrained from deep convection. It should be noted that large-scale sinking motion has recently been observed over a portion of the maritime continent region of the western Pacific (Sherwood 2000), which is also the region where tropopause cirrus is most prevalent (Wang et al. 1996). A possible explanation for this apparent discrepancy is that horizontal transport through this exceptionally cold region leads to cirrus formation in air parcels that reached the cold-point tropopause at other longitudes, where the cold-point temperature is higher (Holton and Gettelman 2001).

In addition to its applicability to the tropopause cirrus problem, the large-scale rising motion mentioned above is also of great interest for the phenomenon of the Brewer–Dobson circulation (Brewer 1949; Dobson 1956; Holton et al. 1995; Rosenlof 1995; Plumb and Eluszkiewicz 1999). Figure 9 is a partial reproduction of Fig. 9 in Mote et al. (1998), which shows a profile of the

mean vertical velocity in the tropical (15°S to 15°N) upper troposphere and lower stratosphere estimated using a time series of satellite measurements of water vapor and methane. This profile shows the equatorial rising branch of the Brewer–Dobson circulation, with a maximum in the rate of ascent of about 0.35 mm s⁻¹ at an altitude of about 18 km, decreasing to a minimum of about 0.2 mm s⁻¹ at about 20 km, and then increasing with altitude in the stratosphere. Of primary interest to this study is the local maximum across the tropical tropopause, which not only constitutes the rising branch of the Brewer–Dobson circulation, but also is potentially able to provide the required moisture transport.

The processes responsible for this tropical upwelling, however, are not well understood. It is partially driven by extratropical “wave drag” (Plumb and Eluszkiewicz 1999; Holton et al. 1995; Rosenlof 1995; Dickinson 1968; Eliassen 1951) in the extratropical stratosphere and mesosphere. However, numerical model experiments by Plumb and Eluszkiewicz (1999) suggest that extratropical wave forcing alone is unable to produce tropical upwelling of the observed magnitude. They found that to generate upwelling of reasonable magnitude the equatorward edge of the stratospheric region of divergence used to represent extratropical wave drag was required to be unrealistically close to the equator, for example, at a latitude near 12°. This result, however, comes from steady-state responses to steady wave drag. Different model responses result if one considers a time-varying wave drag. Holton et al. (1995) show that when the timescale of the wave drag is comparable to that of the radiative relaxation, tropical upwelling takes place even when the equatorward edge of the wave drag is poleward of 20°. Thus, seasonality of the stratospheric wave drag may be the key to the observed tropical upwelling. On the other hand, it is still possible that other mechanisms also contribute to the generation of rising motion in the tropical upper troposphere. If so, it is highly likely that the same mechanisms also transport moisture to the cold-point tropopause. One such alternative mechanism is the focus of this article.

In the mechanism under consideration, rising motion is generated in response to momentum transport by Rossby waves generated by tropical convection. This mechanism is detailed in section 2. In section 3 a large-scale dynamical model used to test this mechanism is described. Sections 4 and 5 describe model runs testing the mechanism. Finally, in section 6 the implications of this work for tropical upwelling and tropopause cirrus are discussed.

2. Hypothesis

In the mechanism under consideration, rising motion is generated in response to the meridional convergence of zonal Rossby wave momentum (eddy momentum flux convergence, hereafter) in the tropical upper troposphere. Tropical Rossby waves can be readily excited

by the zonally asymmetric component of the diabatic heating associated with tropical convection (Gill 1980). Under favorable conditions, these waves are able to propagate poleward into the extratropics (Hoskins and Karoly 1981; Sardeshmukh and Hoskins 1988). Provided that the meridional gradient of the background potential vorticity is positive, there must be meridional convergence of zonal wave momentum into the latitude of the wave source (Held 1975). As the waves propagate away from their source region, wave breaking, nonlinearity, and other dissipation mechanisms including friction dampen the wave flux. The result is meridional divergence of the zonal wave momentum away from the source region. Thus, Rossby waves that are generated in the Tropics (midlatitudes) must pump westerly momentum into (away from) the Tropics. To understand this, consider the zonal-mean zonal momentum equation written in log-pressure coordinates¹:

$$\frac{\partial \bar{u}}{\partial t} + \bar{v} \left[\frac{1}{a \cos \phi} \frac{\partial}{\partial \phi} (\bar{u} \cos \phi) - f \right] + \bar{w} \frac{\partial \bar{u}}{\partial z} = S_x^{(y)} + D, \quad (1)$$

where $S_x^{(y)} = -(1/a \cos^2 \phi)(\partial/\partial \phi)(\overline{u'v'}) \cos^2 \phi$, a is the radius of the earth, ϕ is latitude, D represents appropriate body forces in the longitudinal direction, and the remaining notation is standard. As will be discussed in section 3, in our calculation D represents subgridscale mixing. The vertical convergence of zonal momentum flux is neglected in (1) as this term is much smaller than the meridional convergence of zonal momentum flux, $S_x^{(y)}$, (Lee 1999). As can be seen in (1), there must be westerly wind acceleration in the region where $S_x^{(y)}$ is positive, as long as the collective effect of D and advection of the zonal-mean angular momentum is smaller than $S_x^{(y)}$.

Analyzing 16 yr of National Centers for Environmental Prediction–National Center for Atmospheric Research (NCEP–NCAR) reanalysis data, Lee (1999) showed that the net eddy momentum flux convergence, $S_x^{(y)}$, is indeed positive in the equatorial upper troposphere, indicating that in this region the wave momentum fluxes of tropical-origin dominate those of midlatitude-origin.² Furthermore, it was shown that the spatial and temporal scales of the waves that are responsible

for the momentum flux convergence are consistent with those of the El Niño–Southern Oscillation (ENSO) and the Madden–Julian Oscillation (MJO; Madden and Julian 1971, 1972). This result suggests that the eddy momentum flux convergence in the tropical upper troposphere is ultimately driven by convective heating. As will be argued below, this is the central part of the hypothesis to be tested in this study.

The vertical cross sections of the eddy momentum flux convergence fields, $S_x^{(y)}$, (Figs. 3a–d) show that while the tropical eddy momentum flux convergence is relatively weak, it is present in all seasons. A closer examination of the latitude and altitude of the regions of tropical eddy momentum flux convergence reveals that they are centered near the latitude of the intertropical convergence zone (ITCZ) and the altitude of the convective tropopause, below which nearly all convection is capped.

If gradient wind balance and hydrostatic balance adequately describe the lowest order force balance of the large-scale zonal mean circulation in the tropical atmosphere, the following “thermal wind” relationship must be maintained:

$$\left(f + \frac{2\bar{u} \tan \phi}{a} \right) \frac{\partial \bar{u}}{\partial z} = -\frac{R}{aH} \frac{\partial \bar{T}}{\partial \phi}, \quad (2)$$

where the notation is the same as in (1) with the addition of R for the ideal gas constant and H for the density-scale height. An appropriate momentum and/or heat source in the system can upset thermal wind balance. In response to a vertically localized zonal momentum source, such as that shown in Fig. 3, meridionally overturning circulations, or mean meridional circulations (MMCs), must develop to bring the atmosphere back to a balanced state. This process partially drives the tropospheric MMCs (i.e. the Hadley, Ferrel, and polar cells) and is responsible for the “extratropical pumping” (Holton et al. 1995) of the Brewer–Dobson circulation.

In the case of extratropical pumping, it is the wave drag (westward acceleration of the zonal mean flow) in the subtropical lower stratosphere, also known as the “surf zone,” that upsets the thermal wind balance. In an attempt to restore a balanced state, an MMC develops with a rising branch in the Tropics and subtropics and a sinking branch in high latitudes. This MMC is confined below the altitude of the subtropical surf zone, as friction at the lower boundary balances the Coriolis torque associated with the meridional flow, while such friction does not exist at the upper boundary. This is the essence of “downward control” discussed by Haynes et al. (1991), and succinctly summarized by Plumb and Eluszkiewicz (1999). Because this MMC is shown to be able to account for the bulk of the Brewer–Dobson circulation, the wave drag in the surf zone is accepted as the major driving mechanism of the Brewer–Dobson circulation, although the equatorial upwelling

¹ While we will be using a σ -coordinate model, for conceptual clarity and for the ease of comparison with previous studies (Rosenlof 1995; Plumb and Eluszkiewicz 1999; Andrews et al. 1987) these equations are written in log-pressure coordinates.

² Provided that the meridional potential vorticity gradient is positive, the direction of the eddy momentum flux is opposite to that of the meridional group velocity. Thus, in a wave source latitude where the group velocity diverges, the eddy momentum flux is expected to converge. Also, if the meridional potential vorticity gradient is positive, away from the source latitudes where nonlinear and/or damping effects become important, eddy momentum flux diverges. Therefore, the fact that there is a net convergence of eddy momentum flux in the Tropics suggests that Rossby waves of tropical origin dominate the eddy momentum flux convergence in the Tropics.

driven by that “extratropical pump” appears to be too weak to explain the observed equatorial upwelling. As stated earlier, in their calculations, Plumb and Eluszkiewicz (1999) find that for steady wave drag realistic equatorial upwelling velocity can be obtained only if the drag that mimics the surf zone wave drag intrudes far into the Tropics.

While not widely noted, the tropical upper-tropospheric eddy momentum flux convergence (“tropical wave forcing”, hereafter³) shown in Fig. 3 can also drive an MMC. Furthermore, we argue that the MMC can be driven *above*, as well as below, the level of the tropical wave forcing. Raising the possibility of “upward control” in the tropical atmosphere is not new. Plumb and Eluszkiewicz (1999) points out the importance of weak viscosity in the tropical atmosphere. Their equatorial β -plane scaling analysis predicts that within a tropical internal boundary layer, even weak viscosity is able to balance the zonal component of the Coriolis torque due to the MMC. This tropical internal boundary layer can be as wide as 17° latitude when the ratio of the dissipation rates of zonal momentum to that of thermal anomalies is as small as 0.02; if the dissipation timescale of the thermal anomaly is 10 days, that of the zonal momentum by the viscosity is 500 days. From tracer measurements, Mote et al. (1996) estimate the upper limit of the diffusive timescale to be 7–9 months between 100 and 46 hPa. Combined with the vertical scale of the tracer profile, the vertical diffusivity of the tracer in this layer is estimated as between 0.03 and $0.07 \text{ m}^2 \text{ s}^{-1}$. This is greater than the upper limit of $0.01 \text{ m}^2 \text{ s}^{-1}$ estimated by Hall and Waugh (1997), but smaller than the value of $0.2 \text{ m}^2 \text{ s}^{-1}$ given in WMO (1985). Even with Hall and Waugh’s (1997) relatively lower estimate, the diffusive timescale should not be much greater than 500 days. Thus, assuming that the viscosity of the atmosphere is comparable to the diffusivity of the tracers, the above estimates of diffusivity suggest that upward control in the tropical atmosphere is indeed a good possibility.

Having argued that even weak viscosity can act as a drag that can balance the Coriolis torque associated with the MMC, we now turn to the circulation driven by the tropical wave forcing. Above the level of the tropical wave forcing, this forcing must lessen vertical shear of the zonal wind. In response to this wave forcing, to recover the thermal wind balance expressed by (2), the equator-to-pole temperature gradient must be decreased. In the absence of eddy heat fluxes and diabatic heating, this must be accomplished through adiabatic cooling (warming) equatorward (poleward) of the wave forcing. Thus, above the level of the tropical wave forcing, rising (sinking) motion must be driven equatorward (pole-

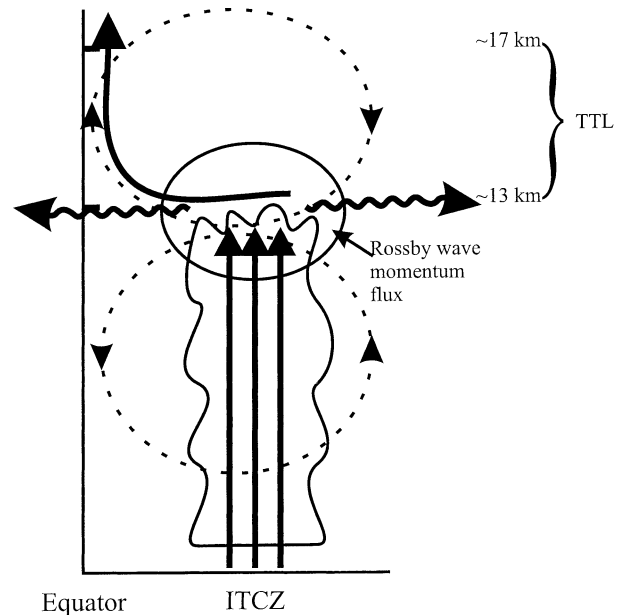


FIG. 1. Summary of the roles played by tropical convection in moisture transport to the cold-point tropopause. First, the convection transports moisture from the surface to the base of the tropopause transition layer (TTL, thick straight arrows). Asymmetry in the diabatic heating associated with the convection excites Rossby waves that propagate away from the ITCZ to both the north and south (direction of propagation indicated by thick wavy arrows). The eddy momentum flux convergence (solid oval) associated with these Rossby waves generates an MMC in the Tropics (dotted arrows). This MMC plays an important role in the transport of moisture toward the equator and upward toward the cold-point tropopause (thick curved arrow).

ward) of the wave forcing. Below the level of the tropical wave forcing, the same argument requires sinking (rising) motion equatorward (poleward) of the wave forcing. Figure 1 shows a schematic diagram of this circulation. For reasons to be explained below, this diagram is drawn for the nonequinoctial condition. A convective cloud is also included in this figure.

Two features of the circulation just described need to be emphasized here. First, rising motion is generated in the equatorial tropopause transition layer (TTL), the region between the convective tropopause and cold-point tropopause. It is this rising motion that is hypothesized both to play a role in the transport of moisture to the cold-point tropopause and to help explain the upper-tropospheric equatorial upwelling of the Brewer–Dobson cell. The overturning circulation above the level of tropical wave forcing provides a mechanism by which moisture detrained from deep convection can be transported to where tropopause cirrus layers are often observed. The equatorward flow within the region of tropical wave forcing plays a role in transporting moisture from the ITCZ, where convection is detraining significant amounts of moisture, to near the equator. Rising motion within the equatorial TTL then transports the moisture vertically to near the cold-point tropopause

³ Referring to the eddy momentum flux convergence as “forcing” is misleading. However, this term is adopted here to be used in parallel with the term wave drag, which represents eddy momentum flux divergence.

where it is required for tropopause cirrus formation. The sinking motion below the level of the tropical wave forcing is not of concern, as the upward moisture transport by convection must be strong enough to offset the large-scale sinking motion generated by the tropical wave forcing. Second, notice that even when the ITCZ is off the equator, the associated tropical wave forcing can readily drive rising motion over the equator, providing a robust mechanism for equatorial upwelling and moisture transport.

3. Model description

Our hypothesis asks whether the mean meridional circulation produced in response to tropical momentum flux convergence induced by Rossby waves generated by tropical convection is able to explain the transport of moisture through the depth of the tropical tropopause transition layer. Thus, the natural first step to test this hypothesis is to determine if an axially symmetric model atmosphere, driven by the observed Rossby wave momentum flux convergence, is able to produce the required MMC. Accordingly, we use the axisymmetric version of a multilevel primitive equation model on the sphere; this model is the dynamical core of the Geophysical Fluid Dynamics Laboratory (GFDL) general circulation model (Feldstein 1994; Kim and Lee 2001).

Equations for the vorticity, divergence, and temperature at each vertical level, and for the pressure at the surface were derived by Bourke (1974). In the original PE model, these equations are integrated in spectral space with the spectral representations of the variables truncated at Rhomboidal-30 resolution. As indicated above, this study uses the axisymmetric version of the PE model by setting the spectral coefficients for nonzero zonal wavenumbers to zero. Sigma coordinates were used in the vertical direction, with 60 sigma levels corresponding to a spacing of 1000 m.

The vertical model resolution and values for various model parameters to be described below closely follow those used by Plumb and Eluszkiewicz (1999), who examined the role of stratospheric wave drag in the extratropical “surf zone” in the generation of tropical upwelling. This was motivated by our desire to assess the relative importance of tropical wave “forcing” and stratospheric surf zone wave drag on the generation of tropical upwelling. When the momentum forcing, $S_x^{(y)}$ in (1), takes the form used in their study, our model is able to reproduce their results in terms of the location and magnitude of the tropical upwelling. This gives us reasonable confidence that the response to tropical and subtropical tropospheric momentum forcing in our model can be directly compared with the response to the stratospheric surf zone wave drag studied by Plumb and Eluszkiewicz (1999).

In (1) D stands for subgrid-scale mixing. In the model this mixing is represented by diffusion. A second-order scheme was used for vertical diffusion and a fourth-

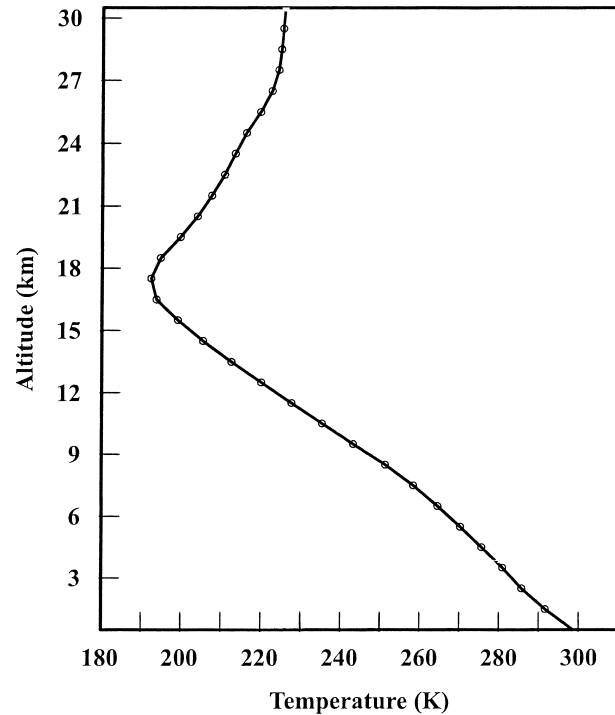


FIG. 2. Zonal-mean temperature profile at the equator for Jan from the NCEP–NCAR reanalysis for the period 1958–97. Used as input temperature profiles for large-scale model runs forced with Jan momentum forcing.

order scheme was used for horizontal diffusion. Except where otherwise indicated, the model runs described here were conducted using a vertical diffusion coefficient of $1.0 \text{ m}^2 \text{ s}^{-1}$ and a biharmonic horizontal diffusion coefficient of $7.0 \times 10^{16} \text{ m}^4 \text{ s}^{-1}$. These values were chosen to ensure computational stability of the numerical model. The sensitivity of our model solution to these somewhat arbitrary diffusion coefficients is described in section 4c.

The upper boundary condition for the model is free slip (no friction), while a linear scheme is used for surface friction at the lower boundary. For the runs considered here a surface friction damping timescale of 1 day is used.

To isolate the MMC that develops in response to momentum forcing from the thermally forced MMC that would result if horizontal gradients were present in the equilibrium temperature field, a horizontally uniform equilibrium temperature field is used. The vertical profile of the equilibrium temperature field used for model runs conducted for January conditions (Fig. 2) is based on the 40-yr mean January equatorial temperature profile from NCEP–NCAR reanalysis data. The altitude of the cold-point tropopause in this profile, 18 km, is consistent with the maximum altitude at which tropopause cirrus is generally observed during Northern Hemisphere winter. Model runs for April, July, and October conditions will also be described. For each of these runs,

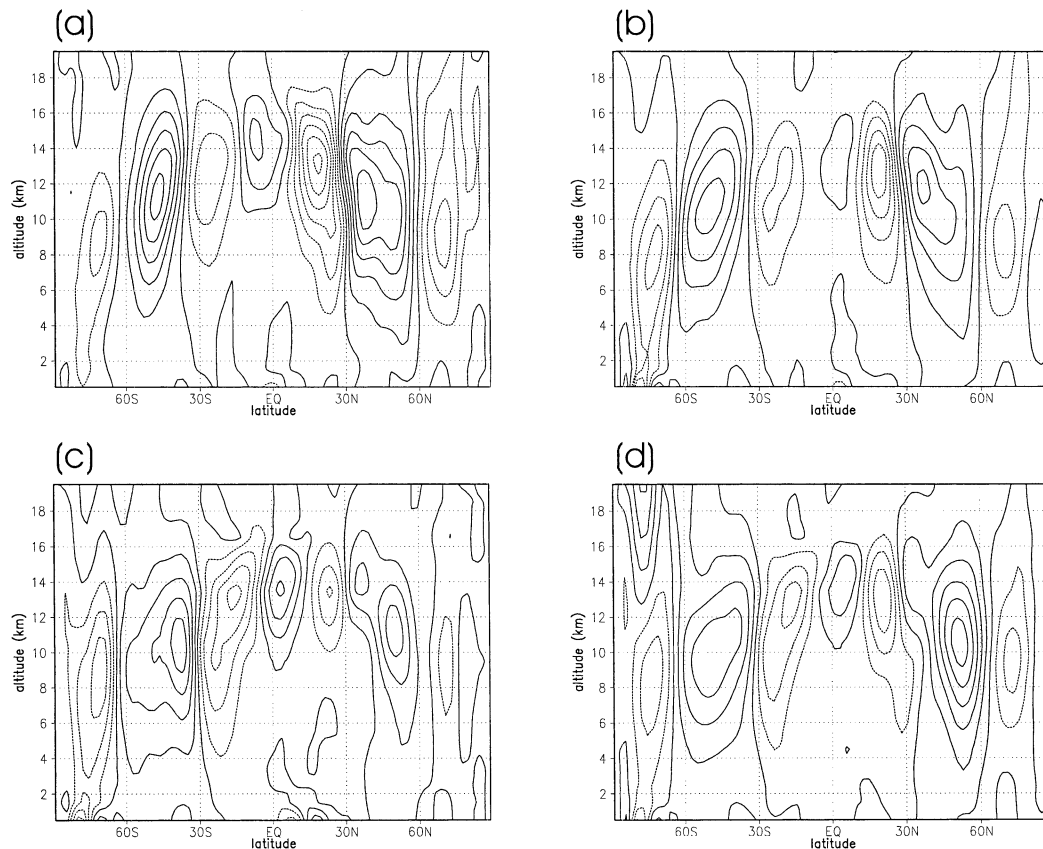


FIG. 3. Monthly and zonal-mean eddy momentum flux convergence fields, calculated based on NCEP–NCAR reanalysis data for the period 1958–97 for the months of (a) Jan, (b) Apr, (c) Jul, and (d) Oct. Positive values indicate momentum flux convergence and negative values (represented by dotted contours) indicate momentum flux divergence. The contour interval is 10^{-5} m s^{-2} .

an equilibrium temperature field based on the 40-yr mean equatorial temperature profile from NCEP–NCAR reanalysis data for the given month is used.

The temperature field is relaxed to the equilibrium temperature field, thereby representing the effects of radiation in maintaining the temperature field. In the stratosphere, radiative processes relax the temperature field to the equilibrium temperature field with a timescale of about 10 days, while in the troposphere, radiative processes are weaker and the relaxation timescale is generally longer, on the order of 20 days. Here, a value of 10 days is used throughout the model domain to prevent the development of strong temperature gradients, again to help isolate the effects of momentum forcing from those of thermal forcing. To test the sensitivity to this parameter, a model run was conducted with a relaxation timescale of 20 days in the troposphere and 10 days in the stratosphere. In this run, the rising motion in the equatorial tropopause transition layer was about 20% stronger than that in the run with a relaxation timescale of 10 days throughout the domain. Thus, the primary qualitative results of this study are not sensitive to this parameter.

In the model runs described here, the model fields

reached steady state after about 200 days of integration. Here, results at the end of 1000 days of integration are presented.

4. Response to January “forcing”

Eddy momentum flux convergence/divergence fields, $S_x^{(y)}$, were calculated based on NCEP–NCAR reanalysis data for the period 1958–97, and were kindly provided by H.-K. Kim of NCEP. The forcing was implemented by adding a term representing acceleration of the zonal-mean wind by momentum flux convergence, $S_x^{(y)}$, to the model zonal momentum equation.

The eddy momentum flux convergence field for January is shown in Fig. 3a. Positive values indicate momentum flux convergence (eastward zonal wind acceleration), while negative values indicate momentum flux divergence (westward zonal wind acceleration). There are three main regions of momentum flux convergence: one in the midlatitudes of each hemisphere and one near the equator. Momentum flux convergence in the midlatitudes is primarily due to momentum transport by extratropical baroclinic disturbances, while momentum flux convergence in the Tropics at the scales resolvable

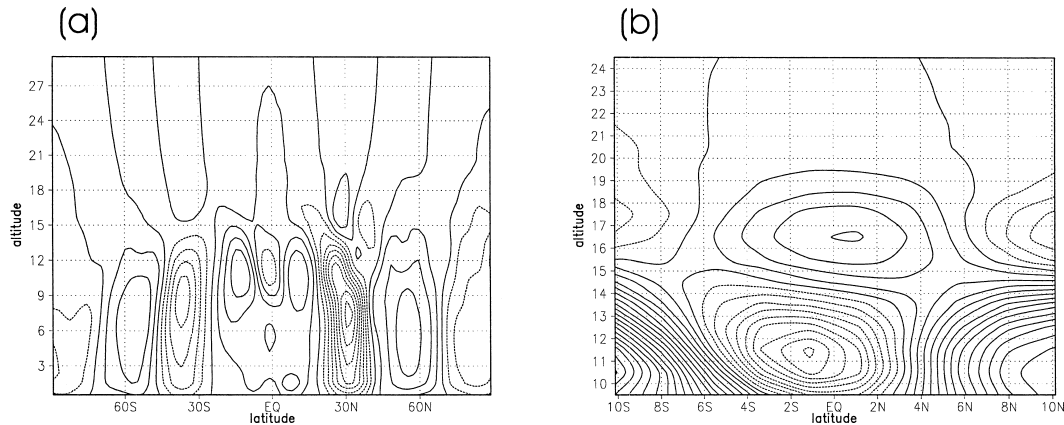


FIG. 4. (a) Vertical velocity field for model run driven by the Jan eddy momentum flux convergence field shown in Fig. 3a. The contour interval is 0.5 mm s^{-1} and negative contours are dotted. (b) Close-up view of this vertical velocity field for the tropical upper troposphere and lower stratosphere. The contour interval has been reduced to 0.1 mm s^{-1} .

by the reanalysis is due to momentum transport by Rossby waves generated by tropical convection (Lee 1999). There are four main regions of momentum flux divergence: one in the subtropics in each hemisphere and one at polar latitudes in each hemisphere. These regions of momentum flux divergence are regions in which Rossby waves tend to break. The feature most relevant to the mechanism under consideration is the tropical region of momentum flux convergence centered at a latitude of 8°S and at an altitude of 14 km. The location of this region is consistent with the mean latitude of the ITCZ during January and with observations that deep convection is generally capped at an altitude of about 14 km.

a. “Control” calculation

Results are now presented for a model run forced with this January momentum flux convergence field. As stated earlier, the values of the diffusion coefficients were $1.0 \text{ m}^2 \text{ s}^{-1}$ for K_V and $7.0 \times 10^{16} \text{ m}^4 \text{ s}^{-1}$ for K_H . The structure of the mean meridional circulation that develops in response to this forcing resembles the observed MMC, as it contains a Hadley cell, a Ferrel cell, and a Polar cell in each hemisphere (Fig. 4a), with each cell being stronger in the Northern Hemisphere than in the Southern Hemisphere due to stronger forcing from baroclinic disturbances in the winter hemisphere than in the summer hemisphere. As expected, the structure of the MMC agrees reasonably well with observations (e.g., Peixoto and Oort 1992) in the midlatitudes, while significant differences are found in the Tropics and subtropics, primarily due to the absence of the thermally driven circulation. This general feature assures the adequacy of our model setup for the investigation at hand.

Because our primary interest is on the rising motion that develops in the tropical tropopause transition layer in response to Rossby wave momentum flux convergence driven by tropical convection, we focus on model

results in the tropical upper troposphere and lower stratosphere. The vertical motion field in this region is shown in Fig. 4b. At the equator, rising motion is observed above about 14 km, with a maximum vertical velocity of about 0.4 mm s^{-1} , or about 35 m day^{-1} , at an altitude of 16.5 km. The magnitude of this rising motion is in good agreement with the estimated vertical velocity in this region (Mote et al. 1998), suggesting that *tropospheric* eddy momentum forcing alone is able to drive the equatorial upwelling in the tropopause transition layer, thereby helping to answer the question as to what is responsible for driving the upwelling across the tropical cold-point tropopause.

b. Relative importance of tropical and midlatitude forcing

If the equatorial upwelling is to effectively transport water vapor, it is desirable that the upwelling be driven by equatorial eddy momentum flux driving rather than by its midlatitude counterpart. The reason is that tropical momentum flux convergence/divergence is driven by Rossby waves excited by tropical convection, and therefore the rising motion generated by this convergence/divergence will be strongest in the vicinity of convection, where it can have the largest impact on moisture transport. In contrast, the equatorial upwelling driven by midlatitude momentum forcing may or may not take place in regions where moisture is readily available to be transported upward.

It would therefore be useful to partition the eddy momentum flux convergence/divergence fields into tropical and extratropical regions, and examine separately the corresponding MMC responses. Accordingly, the total eddy momentum flux convergence/divergence field is partitioned into three portions: the tropical momentum flux convergence (Fig. 5a), the tropical momentum flux convergence plus half of the subtropical divergence (Fig. 5b), and the remaining half of the subtropical di-

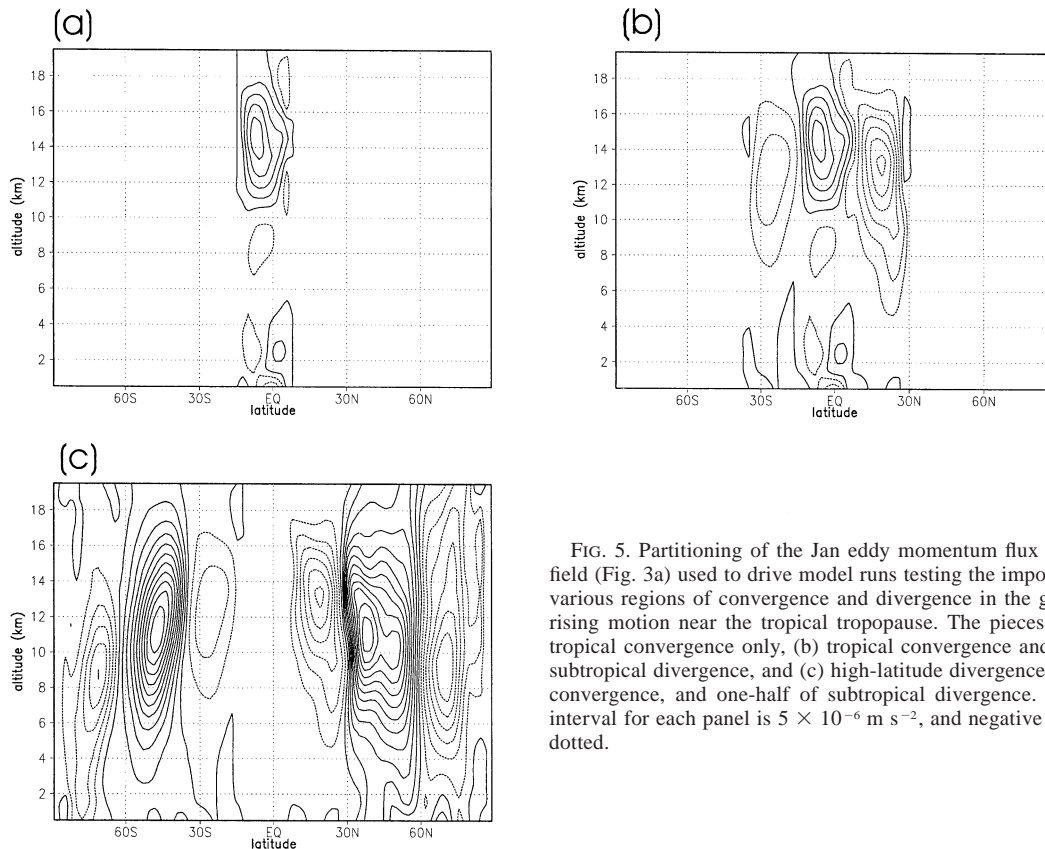


FIG. 5. Partitioning of the Jan eddy momentum flux convergence field (Fig. 3a) used to drive model runs testing the importance of the various regions of convergence and divergence in the generation of rising motion near the tropical tropopause. The pieces include: (a) tropical convergence only, (b) tropical convergence and one-half of subtropical divergence, and (c) high-latitude divergence, midlatitude convergence, and one-half of subtropical divergence. The contour interval for each panel is $5 \times 10^{-6} \text{ m s}^{-2}$, and negative contours are dotted.

vergence plus middle- and high-latitude momentum flux convergence/divergence (Fig. 5c). The sum of Figs. 5b and 5c is equal to Fig. 3a.

Half of the subtropical divergence is included in both Figs. 5b and 5c to crudely represent the subtropical divergence associated with both tropical and midlatitude eddy momentum flux convergence. While a more accurate partitioning of the subtropical divergence could have been calculated, for example, through spectral decomposition (Lee 1999), such detail seems unwarranted given the relatively simple model setup employed here. Furthermore, it will be shown that the tropical eddy momentum flux convergence plays a greater role than subtropical divergence in producing tropical upwelling, so that our conclusions do not depend on the exact partitioning of subtropical divergence.

Figure 6d shows the sum of the model responses to the eddy momentum flux convergence/divergence subsets shown in Figs. 5b and 5c. This solution compares reasonably well with Fig. 4b, indicating that the model response of equatorial upwelling is sufficiently linear. Thus, we now ask what portion of the equatorial upwelling in the full solution (Fig. 4b) is attributable to Rossby waves propagating from the Tropics.

Figure 6a shows the vertical velocity response to the tropical eddy momentum driving shown in Fig. 5a. Within the equatorial TTL, upward vertical velocities

of greater than 0.1 mm s^{-1} are found between 15.5 and 18.5 km, with a peak value of about 0.23 mm s^{-1} at an altitude of about 17 km. Because it is located between the convective tropopause and the cold-point tropopause (Fig. 2), this rising motion is able to assist in the vertical transport of moisture through the TTL. When considering this rising motion, keep in mind that a vertical velocity of 1 mm s^{-1} corresponds to upward motion of about 86 m day^{-1} . Weaker rising motion extends upward into the lower stratosphere.

Now consider a run forced with the sum, shown in Fig. 5b, of the tropical momentum flux convergence and one-half of the subtropical momentum flux divergence. The general features of the vertical velocity field for this run, shown in Fig. 6b, are similar to those in the run forced with only the tropical convergence. Adding the forcing due to subtropical divergence increased the vertical velocity throughout the tropical troposphere, with the amount of the increase decreasing with altitude. In the equatorial upper troposphere, the maximum vertical velocity increased to 0.33 mm s^{-1} .

Finally consider a run forced with the sum, shown in Fig. 5c, of middle- and high-latitude momentum flux convergence and divergence and one-half of the subtropical momentum flux divergence. In this run, the vertical velocity in the tropical upper troposphere and lower stratosphere, shown in Fig. 6c, gradually decreases with

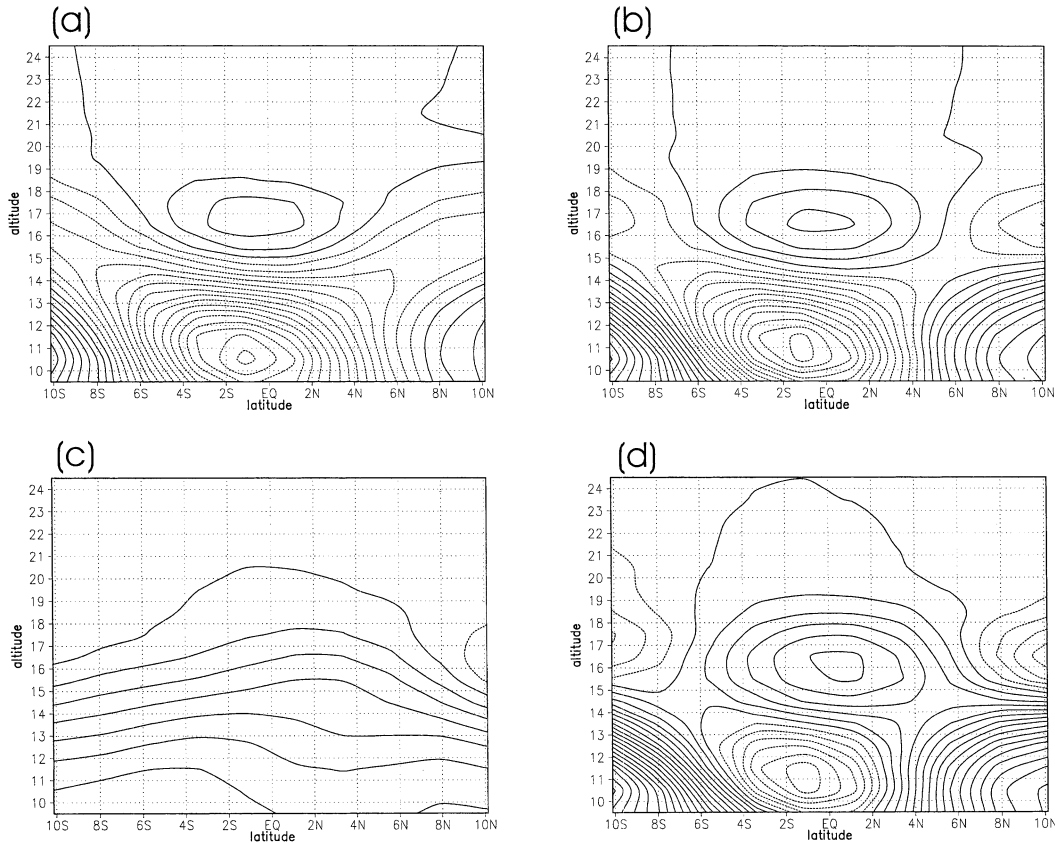


FIG. 6. (a)–(c) Vertical velocity in the tropical upper troposphere and lower stratosphere for model runs driven by the portions of the Jan eddy momentum flux convergence field shown in Figs. 5a–c, respectively. (d) The sum of Figs. 6b and 6c. The contour interval in each panel is 0.1 mm s^{-1} and negative contours are dotted.

height, with a value of about 0.5 mm s^{-1} at an altitude of 12 km decreasing to zero in the lower stratosphere. At 16.5 km, the altitude of the maximum equatorial upwelling associated with tropical momentum flux convergence, the vertical velocity is about 0.2 mm s^{-1} .

The above results suggest that in the zonal mean Rossby waves generated by tropical convection play an equal or slightly greater role in generating rising motion in the TTL than midlatitude disturbances. Both mechanisms generate rising motion within the TTL on the order of 0.2 to 0.3 mm s^{-1} . However, we suspect that the rising motion generated in response to Rossby waves generated by tropical convection is more effective in the vertical transport of moisture through the TTL.

c. Sensitivity

A series of runs forced with January momentum flux convergence were performed to investigate the sensitivity of the modeled tropical upwelling to the values chosen for the diffusion coefficients. First, four runs were conducted in which the second-order vertical diffusion coefficient was set to $1.0 \text{ m}^2 \text{ s}^{-1}$ and the fourth-order horizontal diffusion coefficient was set to 5.0×10^{16} , 7.0×10^{16} , 1.5×10^{17} , and $5.0 \times 10^{17} \text{ m}^4 \text{ s}^{-1}$,

respectively. In each of these runs, the maximum rising motion at the equator was located at an altitude of about 16.5 km, while the vertical velocity at this altitude increased as the coefficient increased, having values of 0.33 , 0.41 , 0.52 , and 0.59 mm s^{-1} , respectively. The vertical upwelling velocity approximately follows logarithmic dependency on the horizontal diffusion coefficient, exhibiting relatively weak sensitivity for values greater than $7.0 \times 10^{16} \text{ m}^4 \text{ s}^{-1}$. In most numerical models like the one used here, the scale-selective horizontal diffusion scheme is included to mimic enstrophy cascade to the subgrid-scales, which results from nonlinear wave interactions. In the calculations presented here, such enstrophy cascade is not present as baroclinic waves are not explicitly represented. On the other hand, inertial instability becomes important in calculations such as those presented here. In fact, weak inertial instability developed in the run with a horizontal diffusion coefficient of $5.0 \times 10^{16} \text{ m}^4 \text{ s}^{-1}$.

Inertial instability has been observed in a number of GCM studies (Dunkerton 1981, 1983, 1989; Hunt 1981; Held and Hou 1980). In the model used for this study, it sometimes develops near the equator, where the Coriolis parameter, f , is small, and near 30°N latitude, where large gradients in the zonal momentum forcing

create large zonal wind gradients. The instability leads to the development of small-scale meridional circulations that act to smooth out the zonal wind gradient. While these small-scale circulations are real solutions to the governing equations, and not just numerical artifacts (Hunt 1981), and the model reaches a steady state in which these circulations are present, the small-scale circulations generated by inertial instability make the model results difficult to interpret. Such an undesirable manifestation of inertial instability can be removed by increasing either the horizontal or vertical diffusion coefficients. Thus, the horizontal diffusion used here may be thought of as mimicking the momentum mixing by the small-scale circulations that are generated by inertial instability. Based on the model runs just described, it was decided to use a value of $7.0 \times 10^{16} \text{ m}^4 \text{ s}^{-1}$ for the fourth-order horizontal diffusion coefficient, except where indicated otherwise. Using this value in association with a vertical diffusion coefficient of $1.0 \text{ m}^2 \text{ s}^{-1}$, the horizontal diffusion is strong enough to decrease the meridional zonal wind gradient to the point where inertial instability virtually disappears.

To test sensitivity to the vertical diffusion coefficient, four model runs were conducted in which the horizontal diffusion coefficient was set to $7.0 \times 10^{16} \text{ m}^4 \text{ s}^{-1}$ and the vertical diffusion coefficient was set to 0.25, 0.5, 1.0, and $2.0 \text{ m}^2 \text{ s}^{-1}$, respectively. The maximum vertical velocity in these runs was again located at an altitude of about 16.5 km, with values at this altitude of 0.47, 0.45, 0.41, and 0.34 mm s^{-1} , respectively. Therefore, the model results are also somewhat sensitive to the vertical diffusion coefficient, with the maximum vertical velocity decreasing by about 25% in response to the factor of 8 increase in the vertical diffusion coefficient. The value of $1.0 \text{ m}^2 \text{ s}^{-1}$ used as the control value is comparable to the values used in some other similar studies (Held and Hou 1980; Lindzen and Hou 1988) and larger than that used by Plumb and Eluszkiewicz (1999). This sensitivity study shows that had a lower value been selected, such as $0.25 \text{ m}^2 \text{ s}^{-1}$ as was used by Plumb and Eluszkiewicz (1999), the magnitude of the tropical upwelling generated by tropical momentum flux convergence would be even larger. In addition, such use of weaker vertical diffusion requires stronger horizontal diffusion, and, as discussed above, increasing the horizontal diffusion coefficient will lead to further strengthening of the vertical upwelling.

These sensitivity studies show that the magnitude of the rising motion in the TTL is somewhat sensitive to the values chosen for the diffusion coefficients, and that the quantitative results of this study should be treated cautiously. However, qualitatively the results are found to be very robust.

In the model runs described here, a thermal relaxation timescale of 10 days is used throughout the model domain to prevent the development of strong temperature gradients. While this value is reasonable in the stratosphere, it is too small in the troposphere by a factor of

about two. As discussed in section 3, a model run conducted using a relaxation timescale of 20 days in the troposphere and 10 days in the stratosphere revealed only minor sensitivity to this parameter, with the main qualitative results basically unaffected.

5. Seasonal dependence of tropical upwelling

The seasonal dependence of tropical upwelling was investigated by conducting model runs forced with the momentum flux convergence fields for the months of January, April, July, and October, shown in Figs. 3a–d. In these fields, the strength and location of the regions of convergence and divergence vary with season. Of the months considered, the tropical momentum flux convergence is strongest during January and July and weakest during April and October. The shift in latitude of the maximum tropical momentum flux convergence is consistent with the observed shift in the location of the mean latitude of the ITCZ from south of the equator during Northern Hemisphere winter to north of the equator during Northern Hemisphere summer. The shift in altitude of the tropical momentum flux convergence is also consistent with the observed seasonal cycle in the altitude of the mean tropical tropopause. The tropical tropopause is highest during Northern Hemisphere winter and lowest during Northern Hemisphere summer (Reid and Gage 1981).

The vertical velocity in the tropical upper troposphere and lower stratosphere for these runs is shown in Fig. 7. In all four months the most prominent feature is the dipole structure of rising (sinking) motion above (below) the tropical momentum flux convergence maximum. In each month, rising motion of greater than 0.3 mm s^{-1} is observed at an altitude of 16 km. These results suggest that tropospheric Rossby wave momentum flux convergence/divergence is able to drive rising motion within the TTL throughout the year.

The relative weakness of the tropical momentum flux convergence in April compared to that in January suggests that the impact of tropical wave momentum flux convergence on rising motion in the TTL would be greater in January than in April. However, a model run forced with only the April tropical momentum flux convergence shows that this is not the case. Figure 8 shows the vertical velocity field for this run. The vertical velocity at the equator above the altitude of maximum forcing is similar in April (Fig. 8) and January (Fig. 6a), while below this altitude the magnitude of the equatorial downwelling is considerably weaker in April than in January. This suggests that the magnitude of the equatorial upwelling generated in response to momentum transport by Rossby waves generated by tropical convection is relatively constant year round.

6. Discussion and concluding remarks

A hypothesis is presented to explain the transport of moisture from where it is detrained from convection to

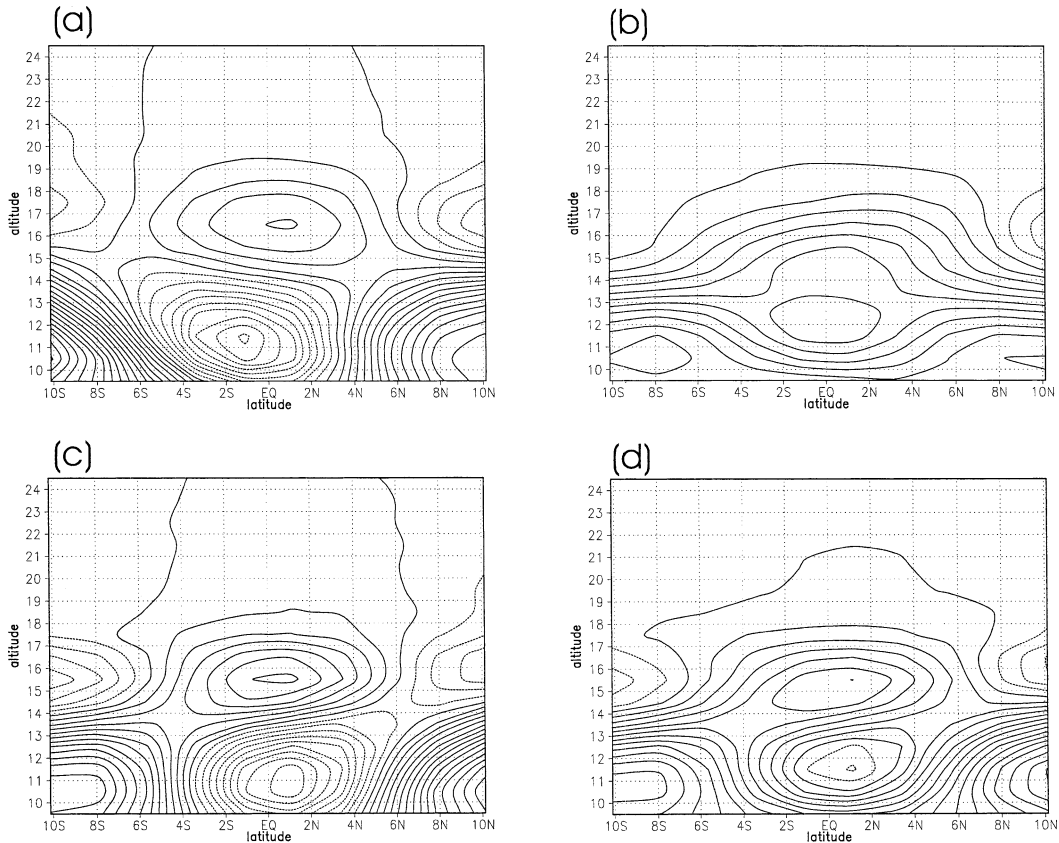


FIG. 7. Vertical velocity in the tropical upper troposphere and lower stratosphere for runs driven by the eddy momentum flux convergence fields for the months shown in Fig. 3. The months shown are: (a) Jan, (b) Apr, (c) Jul, (d) Oct. The contour interval in each panel is 0.1 mm s^{-1} and negative contours are dotted.

the tropical cold-point tropopause, where cirrus layers have been frequently observed. According to this hypothesis, the moisture transport is accomplished by meridionally overturning circulations in the tropical tro-

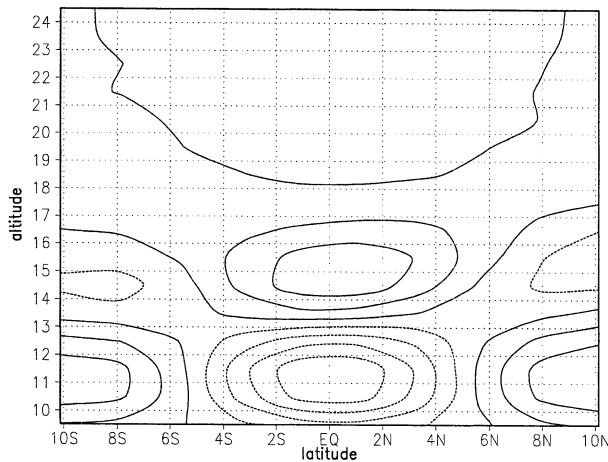


FIG. 8. Vertical velocity in tropical upper troposphere and lower stratosphere for run driven with the tropical region of eddy momentum flux convergence for Apr. The contour interval is 0.1 mm s^{-1} and negative contours are dotted.

popause transition layer that develop in response to momentum transport by Rossby waves generated by tropical convection.

A global primitive equation model has been used to test the hypothesis that Rossby waves generated by tropical convection play a role in the transport of moisture from where it is detrained from convection to the cold-point tropopause. A series of runs was conducted in which the model was driven with fields of eddy momentum flux convergence calculated from NCEP-NCAR reanalysis data.

As is expected from thermal wind adjustment, the output from these model runs shows that Rossby waves generated by tropical convection generate meridionally overturning circulations, including both meridional flow from the ITCZ to the equator and rising motion in the TTL near the equator. It is suggested that the meridional flow plays a role in the transport of moisture from the ITCZ, where it is detrained, to the equator, where tropopause cirrus are often observed; and that the rising motion then transports the moisture vertically through the depth of the TTL to the cold-point tropopause where tropopause cirrus are observed. The meridional transport helps to explain the frequent presence of tropopause cirrus over the equator in spite of the fact that the ITCZ

is rarely positioned there. Note that meridional transport in this region can also be accomplished directly by fluxes associated with the tropical waves themselves. Further work is needed to ascertain the relative importance of these two mechanisms for meridional moisture transport. Additional model runs suggest that the rising motion in the TTL associated with momentum transport by tropical Rossby waves also shows little variation, despite significant seasonal difference in the strength of the tropical forcing (Fig. 3).

Rossby waves also provide meridional heat fluxes. Because the meridional temperature gradient is small in the tropical troposphere, the meridional heat flux is also small for tropical Rossby waves (not shown). For completeness, however, we investigated the impact of this heat flux on the tropical upwelling by forcing the axisymmetric model's temperature equation with the tropospheric zonal-mean meridional heat flux field from the NCEP–NCAR reanalysis data described earlier. The results show that the impact of the heat fluxes in generating rising motion within the tropical TTL is minimal (not shown).

It must be kept in mind that these results were obtained using the axisymmetric version of a primitive equation model. As stated earlier, this is not because we believe that the upwelling takes place in a zonally symmetric manner, but rather because it allows us to test the central idea in a simple dynamical framework. In this version of the model, momentum flux convergence cannot be explicitly resolved, but rather must be prescribed through the addition of a term to the zonal-mean zonal momentum equation. Furthermore, the longitudinal variation of the tropical upwelling (Sherwood 2000; Holton and Gettelman 2001; Pfister et al. 2001) cannot be determined by this model. Therefore, to more completely test and describe the mechanism proposed in this study it is desirable to conduct model runs using the full three-dimensional model. In that direction, one can think of at least two hierarchical model experiments. First, experiments very similar to what was done in this study can be performed, except that full three-dimensional wave momentum flux fields are prescribed. In this case, one expects a three-dimensional circulation as the response. Second, to make a more explicit connection to convection, experiments similar to Highwood and Hoskins (1998) may be performed where an idealized tropical heating, which mimics convective heating, is prescribed. With realistic background flow, the streamfunction response in Highwood and Hoskins (1998) shows structure indicative of Rossby wave propagation into the extratropics. Thus, it is unclear whether the vertical motion field in the upper troposphere and lower stratosphere is understood in terms of the thermal wind adjustment to the baroclinic Rossby wave response (Gill 1980) to the heating (Highwood and Hoskins 1998) or the thermal wind adjustment to the import of westerly momentum from the extratropics, as proposed in our study. We suspect that both mechanisms are operating.

The relative importance of these two processes may be determined by calculating the momentum flux fields resulting from the response to the heating, and repeating the first experiment with this model-generated momentum flux field, rather than with the observed field.

As stated in section 3, to isolate the mean meridional circulation that develops in response to momentum flux convergence from that which would result in the presence of horizontal temperature gradients, a horizontally uniform equilibrium temperature field was used. However, the thermally driven tropical circulation, that is, the Hadley cell, can also leak into the stratosphere (Plumb and Eluszkiewicz 1999). Theoretical calculations by Lindzen and Hou (1988) show that when the maximum diabatic heating associated with tropical convection (corresponds to the ITCZ) lies away from the equator, as is typically observed, the associated rising branch of the Hadley circulation is even farther from the equator [see Fig. 3 in Lindzen and Hou (1988)]. Therefore, although a portion of the rising branch of the Hadley circulation driven by thermal gradients may leak into the TTL, this rising motion is expected to take place *poleward* of the ITCZ. In contrast, the rising motion associated with equatorial momentum flux convergence is focused at the equator (Figs. 1, 4b, and 7), and therefore is expected to play a greater role in the generation of equatorial upwelling than the thermally forced portion of the Hadley circulation.

a. Discussion of Brewer–Dobson tropical upwelling

The results of this study suggest a possible explanation for the tropical vertical velocity profile estimated by Mote et al. (1998) and shown here in Fig. 9. The vertical velocity reaches a local maximum of about 0.35 mm s^{-1} at an altitude of about 17.5 km. Both the magnitude and altitude of this peak approximately agree with the peak vertical velocities determined in the model runs described here (e.g., Fig. 7). Comparing Figs. 7a and 7c more closely, however, one notices that the upwelling response to tropical momentum forcing is greater in July than in January. This contrasts with observations (e.g., Eluszkiewicz et al. 1996) that the tropical upwelling is in general greater in January than in July. We do not yet have an explanation for this discrepancy in seasonal asymmetry, and this is certainly an issue that needs to be addressed in a future study.

Above 18 km, the estimated vertical velocity then decreases with altitude to a value of about 0.2 mm s^{-1} at an altitude of about 20 km, before increasing with altitude in the stratosphere. That there is an upwelling minimum between the TTL and the middle stratosphere suggests that the primary mechanism for the local maximum in the TTL is different than that for the local maximum in the middle stratosphere. In particular, the altitude of the latter suggests that diabatic heating by, say, ozone, might be responsible for the upwelling peak,

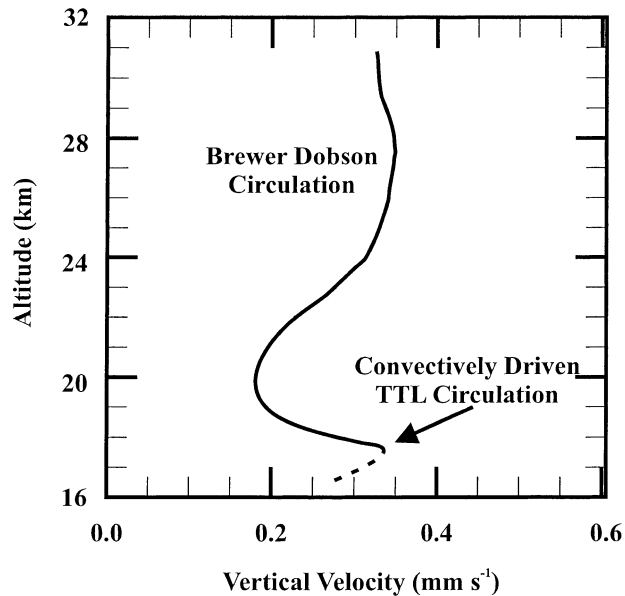


FIG. 9. Vertical velocity in the tropical upper troposphere and stratosphere calculated using measurements of water vapor and methane as tracers. These measurements were obtained from the Upper Atmosphere Research Satellite Halogen Occultation Experiment (adapted from Mote et al. 1998). Note that the portion of the profile indicated by the dotted line is sensitive to assumptions of the profile of vertical diffusion near the tropopause.

while the surf zone wave pump remains as a viable mechanism for the overall observed tropical upwelling.

While the discrepancy in the seasonal asymmetry in the TTL upwelling velocity poses as a potential pitfall, the above consideration leads us to speculate the following picture; the primary mechanism for the local maximum in the TTL is tropical eddy momentum flux convergence associated with Rossby waves generated by tropical convection, the primary mechanism for the local maximum in the middle stratosphere is diabatic heating by ozone, and the surf zone wave pump contributes toward weak background upwelling throughout the entire depth.

b. Implications for tropical tropopause cirrus

As stated earlier, the meridional circulation within the TTL described here suggests a possible explanation for the frequent occurrence of tropopause cirrus over the equator despite the facts that the ITCZ is generally located several degrees away from the equator and tropical convection is almost always capped at least 2 km below the cold-point tropopause where these layers are observed. According to this hypothesis, the equatorward branch of the circulation transports moisture horizontally from the ITCZ to the equator, where the rising branch of the circulation, which is expected to be strongest at the equator, transports the moisture vertically to the cold-point tropopause.

Once moisture is present near the cold-point tropo-

pause, large-scale cooling is required to initiate the ice crystal nucleation and growth that leads to the widespread in situ formation and maintenance of tropopause cirrus. Adiabatic cooling associated with the tropical upwelling under consideration here is one possible source of this large-scale cooling. However other cooling sources likely play more important roles. For example, Boehm and Verlinde (2000) showed close correlation between Kelvin waves in the lower stratosphere (Holton et al. 2001) and cirrus layers near the tropical cold-point tropopause during Nauru99, an Intensive Operational Period conducted by the Department of Energy Atmospheric Radiation Measurement program.

Once tropopause cirrus forms, the atmospheric layer containing the cirrus is typically radiatively heated, and this heating is generally $0.5\text{--}4\text{ K day}^{-1}$ (CAM; McFarquhar et al. 2000). Recently, Thuburn and Craig (2002) showed that radiative warming on the order of 0.2 K day^{-1} in a narrow region near the cold-point tropopause plays a role in creating the tropopause transition layer. While Thuburn and Craig (2002) looked at heating associated with carbon dioxide, we suggest that in regions where tropopause cirrus is prevalent, the heating associated with the cirrus may also play a role in creating the TTL. Above the radiatively warmed layer, the air can become statically unstable, and small-scale convection may take place. Such convection, if it indeed occurs, must cool the layer heated by the cirrus, thereby playing a role in balancing the radiative heating. Clearly, more observational and modeling effort is required to further our understanding of the physical processes associated with tropopause cirrus.

Acknowledgments. We gratefully acknowledge Johannes Verlinde, thesis advisor for MTB, for all of his assistance and guidance during the course of this work, especially in regard to the implications for tropopause cirrus. MTB was supported by a NASA Earth System Science Fellowship. This work was supported in part by a grant from the Department of Energy under the Atmospheric Radiation Measurement program (DE-FB02-90ER6L071). SL was supported by National Science Foundation Grant ATM-0001473.

REFERENCES

- Ackerman, T. P., K.-N. Liou, F. P. J. Valero, and L. Pfister, 1988: Heating rates in tropical anvils. *J. Atmos. Sci.*, **45**, 1606–1623.
- Andrews, D. G., J. R. Holton, and C. B. Leovy, 1987: *Middle Atmospheric Dynamics*. Academic Press, 489 pp.
- Boehm, M. T., and J. Verlinde, 2000: Stratospheric influence on upper tropospheric tropical cirrus. *Geophys. Res. Lett.*, **27**, 3209–3212.
- Boering, K. A., S. C. Wofsy, B. C. Daube, H. R. Schneider, M. Loewenstein, J. R. Podolske, and T. J. Conway, 1996: Stratospheric mean ages and transport rates from observations of carbon dioxide and nitrous oxide. *Nature*, **274**, 1340–1343.
- Booker, D. R., and P. G. Stickel, 1982: High altitude tropical cirrus cloud observations. Preprints, *Conf. on Cloud Physics*, Chicago, IL, Amer. Meteor. Soc., 215–217.

- Bourke, W., 1974: A multi-level spectral model. I. Formulation and hemispheric integrations. *Mon. Wea. Rev.*, **102**, 687–701.
- Brewer, A. W., 1949: Evidence for a world circulation provided by the measurements of helium and water vapor distribution in the stratosphere. *Quart. J. Roy. Meteor. Soc.*, **75**, 351–363.
- Clark, H. L., R. S. Harwood, P. W. Mote, and W. G. Read, 1998: Variability of water vapor in the tropical upper troposphere as measured by the Microwave Limb Sounder on UARS. *J. Geophys. Res.*, **103**, 31 695–31 707.
- Danielsen, E. F., 1993: In situ evidence of rapid, vertical, irreversible transport of lower tropospheric air into the lower tropical stratosphere by convective cloud turrets and by larger-scale upwelling in tropical cyclones. *J. Geophys. Res.*, **98**, 8665–8881.
- Defant, F., and H. M. E. van de Boogaard, 1963: The global circulation features of the troposphere between the equator and 40°N, based on a single day's data. Part 1. The structure of the basic meteorological fields. *Tellus*, **15**, 251–260.
- Dickinson, R. E., 1968: On the excitation and propagation of zonal winds in an atmosphere with Newtonian cooling. *J. Atmos. Sci.*, **25**, 269–279.
- Dobson, G. M. B., 1956: Origin and distribution of the polyatomic molecules in the atmosphere. *Proc. Roy. Soc. London*, **236A**, 187–193.
- Dunkerton, T. J., 1981: On the inertial stability of the equatorial middle atmosphere. *J. Atmos. Sci.*, **38**, 2354–2364.
- , 1983: A nonsymmetric equatorial inertial instability. *J. Atmos. Sci.*, **40**, 807–813.
- , 1989: Nonlinear Hadley circulation driven by asymmetric differential heating. *J. Atmos. Sci.*, **46**, 956–974.
- Ebert, E. E., and G. J. Holland, 1992: Observations of record cold cloud-top temperatures in Tropical Cyclone Hilda (1990). *Mon. Wea. Rev.*, **120**, 2240–2251.
- Eliassen, A., 1951: Slow thermally or frictionally controlled meridional circulation in a circular vortex. *Astrophys. Norv.*, **5** (2), 19–60.
- Elson, L. S., W. G. Read, J. W. Waters, P. W. Mote, J. S. Kinnery, and R. S. Harwood, 1996: Space-time variations in water vapor as observed in the UARS Microwave Limb Sounder. *J. Geophys. Res.*, **101**, 9001–9015.
- Eluszkiewicz, J., and Coauthors, 1996: Residual circulation in the stratosphere and lower mesosphere as diagnosed from microwave limb sounder data. *J. Atmos. Sci.*, **53**, 217–240.
- Feldstein, S. B., 1994: A weakly nonlinear primitive equation baroclinic life cycle. *J. Atmos. Sci.*, **51**, 23–34.
- Folkens, I., M. Loewenstein, J. Podolske, S. J. Oltmans, and M. Proffitt, 1999: A barrier to vertical mixing at 14 km in the Tropics: Evidence from ozonesondes and aircraft measurements. *J. Geophys. Res.*, **104**, 22 095–22 102.
- Forster, P. M. F., R. S. Freckleton, and K. P. Shine, 1997: On aspects of the concept of radiative forcing. *Climate Dyn.*, **13**, 547–560.
- Gettelman, A., M. L. Salby, and F. Sassi, 2002: Distribution and influence of convection in the tropical tropopause region. *J. Geophys. Res.*, **107** (D10), 4080, doi:10.1029/2001JD001048.
- Gill, A. E., 1980: Some simple solutions for heat-induced tropical circulation. *Quart. J. Roy. Meteor. Soc.*, **106**, 447–462.
- Graves, M. E., 1951: The relation between the tropopause and convective activity in the subtropics (Puerto Rico). *Bull. Amer. Meteor. Soc.*, **32**, 54–60.
- Hall, T. M., and D. Waugh, 1997: Tracer transport in the tropical stratosphere due to vertical diffusion and horizontal mixing. *Geophys. Res. Lett.*, **24**, 1383–1386.
- Hartmann, D. L., J. R. Holton, and Q. Fu, 2001: The heat balance of the tropical tropopause, cirrus, and stratospheric dehydration. *Geophys. Res. Lett.*, **28**, 1969–1972.
- Haynes, P. H., C. J. Marks, M. E. McIntyre, T. G. Shepherd, and K. P. Shine, 1991: On the “downward control” of extratropical diabatic circulations by eddy-induced mean zonal forces. *J. Atmos. Sci.*, **48**, 651–678.
- Held, I. M., 1975: Momentum transport by quasi-geostrophic eddies. *J. Atmos. Sci.*, **32**, 1494–1497.
- , and A. Y. Hou, 1980: Nonlinear axially symmetric circulations in a nearly inviscid atmosphere. *J. Atmos. Sci.*, **37**, 515–533.
- Heymsfield, A. J., 1986: Ice particles observed in a cirriform cloud at –83°C and implications for polar stratospheric clouds. *J. Atmos. Sci.*, **43**, 851–855.
- , and G. M. McFarquhar, 1996: High albedos of cirrus in the tropical Pacific warm pool: Microphysical interpretations from CEPEX and from Kwajalein, Marshall Islands. *J. Atmos. Sci.*, **53**, 2424–2451.
- , G. M. McFarquhar, W. D. Collins, J. A. Goldstein, F. P. J. Valero, J. Spinhirne, W. Hart, and P. Pilewskie, 1998: Cloud properties leading to highly reflective tropical cirrus: Interpretations from CEPEX, TOGA COARE, and Kwajalein, Marshall Islands. *J. Geophys. Res.*, **103**, 8805–8812.
- Highwood, E. J., and B. J. Hoskins, 1998: The tropical tropopause. *Quart. J. Roy. Meteor. Soc.*, **124**, 1579–1604.
- Holton, J. R., and A. Gettelman, 2001: Horizontal transport and the dehydration of the stratosphere. *Geophys. Res. Lett.*, **28**, 2799–2802.
- , P. H. Haynes, M. E. McIntyre, A. R. Douglass, R. B. Rood, and L. Pfister, 1995: Stratosphere–troposphere exchange. *Rev. Geophys.*, **33**, 403–439.
- , M. J. Alexander, and M. T. Boehm, 2001: Evidence for short vertical wavelength Kelvin waves in the Department of Energy–Atmospheric Radiation Measurement Nauru99 radiosonde data. *J. Geophys. Res.*, **106**, 20 125–20 129.
- Hoskins, B. J., and D. J. Karoly, 1981: The steady linear response of a spherical atmosphere to thermal and orographic forcing. *J. Atmos. Sci.*, **38**, 1179–1196.
- Hunt, B. G., 1981: The maintenance of the zonal mean state of the upper atmosphere as represented in a three-dimensional general circulation model extending to 100 km. *J. Atmos. Sci.*, **38**, 2172–2186.
- Jensen, E. J., O. B. Toon, L. Pfister, and H. B. Selkirk, 1996a: Dehydration of the upper troposphere and lower stratosphere by subvisible cirrus clouds near the tropical tropopause. *Geophys. Res. Lett.*, **23**, 825–828.
- , —, H. B. Selkirk, J. D. Spinhirne, and M. R. Schoeberl, 1996b: On the formation and persistence of subvisible cirrus clouds near the tropical tropopause. *J. Geophys. Res.*, **101**, 21 361–21 375.
- Keith, D. W., 2000: Stratosphere–troposphere exchange: Inferences from the isotopic composition of water vapor. *J. Geophys. Res.*, **105**, 15 167–15 173.
- Kim, H.-K., and S. Lee, 2001: Hadley cell dynamics in a primitive equation model. Part I: Axisymmetric flow. *J. Atmos. Sci.*, **58**, 2845–2858.
- Kley, D., A. L. Schmeltekopf, K. Kelly, R. H. Winkler, T. L. Thompson, and M. McFarland, 1982: Transport of water through the tropical tropopause. *Geophys. Res. Lett.*, **9**, 617–620.
- Knollenberg, R. G., A. J. Dascher, and D. Huffman, 1982: Measurements of the aerosol and ice crystal populations in tropical stratospheric cumulonimbus anvils. *Geophys. Res. Lett.*, **9**, 613–616.
- Lee, S., 1999: Why are the climatological zonal winds easterly in the equatorial upper troposphere? *J. Atmos. Sci.*, **56**, 1353–1363.
- Lindzen, R. S., and A. V. Hou, 1988: Hadley circulations for zonally averaged heating centered off the equator. *J. Atmos. Sci.*, **45**, 2416–2427.
- Madden, R. A., and P. R. Julian, 1971: Detection of a 40–50 day oscillation in the zonal wind in the tropical Pacific. *J. Atmos. Sci.*, **28**, 702–708.
- , and —, 1972: Description of global-scale circulation cells in the Tropics with a 40–50 day period. *J. Atmos. Sci.*, **29**, 1109–1123.
- Mather, J. H., T. P. Ackerman, and M. P. Jensen, 1998: Characteristics of the atmospheric state and the surface radiation budget at the tropical western Pacific ARM site. *Geophys. Res. Lett.*, **25**, 4513–4516.
- McFarquhar, G. M., A. J. Heymsfield, J. Spinhirne, and B. Hart, 2000:

- Thin and subvisual tropopause tropical cirrus: Observations and radiative impacts. *J. Atmos. Sci.*, **57**, 1841–1853.
- Mote, P. W., and Coauthors, 1996: An atmospheric tape recorder: The imprint of tropical tropopause temperatures on stratospheric water vapor. *J. Geophys. Res.*, **101**, 3989–4006.
- , T. J. Dunkerton, M. E. McIntyre, E. A. Ray, P. H. Haynes, and J. M. Russell III, 1998: Vertical velocity, vertical diffusion, and dilution by midlatitude air in the tropical lower stratosphere. *J. Geophys. Res.*, **103**, 8651–8666.
- Newell, R. E., and S. Gould-Stewart, 1981: A stratospheric fountain? *J. Atmos. Sci.*, **38**, 2789–2796.
- Niwano, M., and M. Shiotani, 2001: Quasi-biennial oscillation in vertical velocity inferred from trace gas data in the equatorial lower stratosphere. *J. Geophys. Res.*, **106**, 7281–7290.
- Palmén, E., and C. W. Newton, 1969: *Atmospheric Circulation Systems: Their Structure and Interpretation*. Academic Press, 603 pp.
- Peixoto, J. P., and A. H. Oort, 1992: *Physics of Climate*. American Institute of Physics, 520 pp.
- Pfister, L., and Coauthors, 2001: Aircraft observations of thin cirrus clouds near the tropical tropopause. *J. Geophys. Res.*, **106**, 9765–9786.
- Plumb, R. A., and J. Eluszkiewicz, 1999: The Brewer–Dobson circulation: Dynamics of the tropical upwelling. *J. Atmos. Sci.*, **56**, 868–890.
- Potter, B. E., and J. R. Holton, 1995: The role of monsoon convection in the dehydration of the lower tropical stratosphere. *J. Atmos. Sci.*, **52**, 1034–1050.
- Reid, G. C., and K. S. Gage, 1981: On the annual variation in height of the tropical tropopause. *J. Atmos. Sci.*, **38**, 1928–1938.
- Rosenfield, J. E., D. B. Considine, M. R. Schoeberl, and E. V. Browell, 1998: The impact of subvisible cirrus clouds near the tropical tropopause on stratospheric water vapor. *Geophys. Res. Lett.*, **25**, 1883–1886.
- Rosenlof, K. H., 1995: Seasonal cycle of the residual mean meridional circulation in the stratosphere. *J. Geophys. Res.*, **100**, 5173–5191.
- , and J. R. Holton, 1993: Estimates of the stratospheric residual circulation using the downward control principle. *J. Geophys. Res.*, **98**, 10 465–10 479.
- Rossow, W. B., and R. A. Schiffer, 1991: ISCCP cloud data products. *Bull. Amer. Meteor. Soc.*, **72**, 2–20.
- Salathé, E. P., Jr., and D. L. Hartmann, 1997: A trajectory analysis of tropical upper-tropospheric moisture and convection. *J. Climate*, **10**, 2533–2547.
- Sardeshmukh, P. D., and B. J. Hoskins, 1988: The generation of global rotational flow by steady idealized tropical divergence. *J. Atmos. Sci.*, **45**, 1228–1251.
- Schmetz, J., S. A. Tjemkes, M. Gube, and L. van de Berg, 1997: Monitoring deep convection and convective overshooting with Meteosat. *Adv. Space Res.*, **19**, 433–441.
- Seol, D.-I., and K. Yamazaki, 1999: Residual mean meridional circulation in the stratosphere and upper troposphere: Climatological aspects. *J. Meteor. Soc. Japan*, **77**, 985–996.
- Sherwood, S. C., 1999: On moistening of the tropical troposphere by cirrus clouds. *J. Geophys. Res.*, **104**, 11 949–11 960.
- , 2000: A stratospheric “drain” over the maritime continent. *Geophys. Res. Lett.*, **27**, 677–680.
- , and A. E. Dessler, 2000: On the control of stratospheric humidity. *Geophys. Res. Lett.*, **27**, 2513–2516.
- , and —, 2001: A model for transport across the tropical tropopause. *J. Atmos. Sci.*, **58**, 765–779.
- Simpson, J., J. Halverson, H. Pierce, C. Morales, and T. Iguchi, 1998: Eyeing the eye: Exciting early stage science results from TRMM. *Bull. Amer. Meteor. Soc.*, **79**, 1711.
- Thuburn, J., and G. C. Craig, 1997: GCM tests of theories for the height of the tropopause. *J. Atmos. Sci.*, **54**, 869–882.
- , and —, 2002: On the temperature structure of the tropical stratosphere. *J. Geophys. Res.*, **107** (D2), 4017, doi:10.1029/2001JD000448.
- Tsuda, T., Y. Murayama, H. Wiryosumarto, S. W. B. Harijono, and S. Kato, 1994: Radiosonde observations of equatorial atmosphere dynamics over Indonesia. I. Equatorial waves and diurnal tides. *J. Geophys. Res.*, **99**, 10 491–10 505.
- Wang, P.-H., P. Minnis, M. P. McCormick, G. S. Kent, and K. M. Skeens, 1996: A 6-year climatology of cloud occurrence frequency from Stratospheric Aerosol and Gas Experiment II observations (1985–1990). *J. Geophys. Res.*, **101**, 29 407–29 429.
- Winker, D. M., and C. R. Trepte, 1998: Laminar cirrus observed near the tropical tropopause by LITE. *Geophys. Res. Lett.*, **25**, 3351–3354.
- WMO, 1985: Atmospheric ozone. Rep. 16, Global Ozone Research and Monitoring Project, World Meteorological Organization, 1095 pp.